ISBN: 978-3-95450-248-6 ISSN: 2673-5490 doi: 10.18429/JACoW-IPAC2025-TUPM026

ADVANCED BEAM TUNING AND BEAM MEASUREMENTS TECHNIQUES IN THE CLEAR FACILITY

A. Petersson^{1,2,†}, A. Aksoy¹, L. Bonnard¹, R. Corsini¹, W. Farabolini¹, O. Franek^{1,3}, D. Gamba¹, E. Granados¹, A. Gilardi¹, P. Korysko^{1,4}, A. Malyzhenkov^{1.5}, V. Rieker^{1, 6}, K. N. Sjøbæk⁶, G. Tangari^{1,7}, L. M. Wroe¹ ¹European Organization for Nuclear Research CERN, Geneva, Switzerland ²Lund University, Lund, Sweden ³Czech Technical University in Prague, Prague, Czech Republic ⁴University of Oxford, Oxford, UK ⁵Swiss International Institute Lausanne, Prilly, Switzerland ⁶University of Oslo, Oslo, Norway ⁷Sapienza University of Rome, Rome, Italy

Abstract

The CLEAR (CERN Linear Electron Accelerator for Research) facility delivers to a wide user community a 200 MeV electron beam with highly flexible parameters. Running conditions range from single-bunch to multi-bunch operation, with bunch charges from 10 pC to 1 nC, bunch durations from 100 fs to tens of ps, and includes tunable momentum (30 MeV/c to 220 MeV/c). Such a variety of beam conditions poses a challenge to the beam instrumentation and to the beam measurements and tuning techniques, even more so given that quite often a rapid switch from one set of conditions to a very different one is required. In this paper we present several examples of the techniques developed in CLEAR for this purpose and discuss their advantages and limitations. Examples include emittance measurements and phase space reconstruction procedures by quadrupole scans and beam based alignment methods.

INTRODUCTION

The CERN Linear Electron Accelerator for Research (CLEAR) is a versatile test facility at CERN, delivering a highly tunable beam to experiments for beam instrumentation, novel acceleration schemes, radiation-effect studies on electronics and medical applications [1–3].

Accurate knowledge of beam parameters is essential for many of these studies, and screen-based imaging provides a fundamental measurement tool. Such measurements demand precise calibration and robust image processing routines, whose implementation is detailed in this paper along with the application of these image processing techniques to quadrupole scans. The same techniques have also been leveraged in studies of beam-based alignment.

SCREEN IMAGING SYSTEM

The CLEAR beamline houses a total of seven in-vacuum screens for beam imaging. Of these screens, five use Ceriumdoped Yttrium Aluminum Garnet (YAG), one uses Optical Transition Radiation (OTR) and one has the option to switch

between YAG and OTR screens. The use of these screens for beam based measurements requires careful calibration and image processing.

Homographic Calibration

Six of the screens are inclined at 45° from the beam axis, creating a large perspective distortion. This motivates the use of homography for perspective correction. Given the image pixel coordinates x_p, y_p , the coordinates x, y relative to the beam axis are given by [4]:

$$s \begin{bmatrix} x \\ y \\ 1 \end{bmatrix} = H \begin{bmatrix} x_p \\ y_p \\ 1 \end{bmatrix}, \tag{1}$$

where H is the homography matrix and s is used to normalize the third vector component, implicitly introducing non-linearity. The matrix for each screen can be calculated by mapping the pixel coordinates of calibration markers on the screens to beam coordinates [4], taking into account the screen angle. The transformation can also be approximated by linearizing the homographic transformation around the center of the screen, which can be used to create simple pixel size and pixel offset calibrations for older software that cannot use the full homographic transformation.

Image Handling for Beam Based Measurements

Due to the flexible nature of CLEAR, the beam can vary dramatically in size, position and shape on the screens. It is therefore paramount that the method for measuring these quantities is both robust and flexible. The image handling consists of

- 1. An initial crop to remove screen bezels.
- 2. Background subtraction of an average of five images without beam.
- 3. Filtering using a 3×3 median filter to remove salt-andpepper noise while preserving image features.
- 4. A rectangular region of interest containing the beam is automatically calculated, cropping it at 5 % of the maximum amplitude.

[†] email: alfred.petersson@cern.ch

The mean position of the beam, its variance and covariance are then calculated using the pixel amplitudes of the treated image in the region of interest using:

$$\bar{x} = \sum_{i} w_i x_i,\tag{2}$$

$$\sigma_x^2 = \sum_i w_i (x_i - \bar{x})^2, \tag{3}$$

$$\sigma_{xy} = \sum_{i} w_i (x_i - \bar{x}) (y_i - \bar{y}), \tag{4}$$

where for each pixel i, w_i is the normalized pixel amplitude and x_i , y_i are pre-calculated coordinates given by the homography matrix.

Resolution Limit

The smallest measurable beam size is given by the resolution limit of both the imaging system (due to sensor and lens properties) and the light emission of the screen. For a beam with standard deviation σ , the resolution limit of the imaging system σ_i and screen σ_s will contribute to an increase of the measured beam standard deviation σ_m given by [5]:

$$\sigma_m^2 = \sigma^2 + \sigma_r^2,\tag{5}$$

where $\sigma_r^2 = \sigma_i^2 + \sigma_s^2$ is the combined resolution limit.

The resolution σ_i of one of the CLEAR imaging systems was measured to roughly 30 µm using line pair resolution tests. The resolution limit of the screen light emission varies based on the type of screen (YAG or OTR), and for YAG screens also increases with screen thickness [6]. The YAG screens used in CLEAR are 500 µm thick, resulting in a large σ_s being the dominant effect. To model the uncertainty $\delta\sigma$ in the beam size, the sample standard deviation of the mean $\delta\sigma_m$ of the measured beam size and the uncertainty $\delta\sigma_r$ in σ_r is propagated as:

$$\delta\sigma = \sqrt{\left(\frac{\sigma_m \delta\sigma_m}{\sigma}\right)^2 + \left(\frac{\sigma_r \delta\sigma_r}{\sigma}\right)^2}.$$
 (6)

Due to the difficulty in estimating the true resolution limit, σ_r and $\delta\sigma_r$ of each screen was modeled as the mean and standard deviation of a uniform distribution with the pixel resolution as a lower bound and the minimum achieved beam size measurement as an upper bound.

QUADRUPOLE SCANS

Using the image handling procedure described in the previous section, a software tool for quadrupole scans was implemented. The tool uses the statistical definitions of the normalized emittance ε and Twiss parameters β , α , γ [7]:

$$\frac{\varepsilon}{\beta_z \gamma_z} \begin{bmatrix} \beta & -\alpha \\ -\alpha & \gamma \end{bmatrix} = \begin{bmatrix} \langle u^2 \rangle & \langle uu' \rangle \\ \langle uu' \rangle & \langle u'^2 \rangle \end{bmatrix}, \tag{7}$$

$$\frac{\varepsilon}{\beta_z \gamma_z} = \sqrt{\begin{vmatrix} \langle u^2 \rangle & \langle uu' \rangle \\ \langle uu' \rangle & \langle u'^2 \rangle \end{vmatrix}},\tag{8}$$

where β_z is the relativistic beta and γ_z the Lorentz factor.

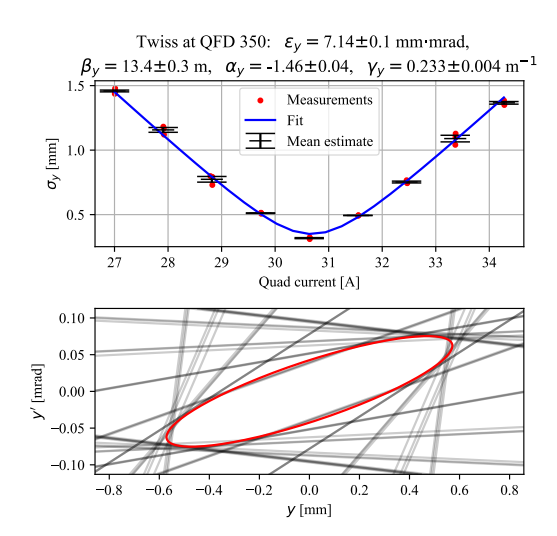


Figure 1: Results of a quadrupole scan taken with the new software. Top: The measurement points and χ^2 -fit. Bottom: The estimated one-sigma ellipse in phase space, showing the constraint given by each measurement point as a black line.

The quadrupole scan tool allows the user to scan a single quadrupole over a linear range of current setpoints, keeping the remaining quadrupoles constant. The code is developed with extension to more complex scans using multiple quadrupoles in mind, as described in Ref. [8]. A linear lattice is constructed for each setpoint of the quadrupole current and the Twiss matrix formulation is used to compute a 3×3 matrix M_i [9] for each quadrupole setting i such that:

$$\begin{bmatrix} \beta \\ \alpha \\ \gamma \end{bmatrix} = M_i \begin{bmatrix} \beta_0 \\ \alpha_0 \\ \gamma_0 \end{bmatrix} \tag{9}$$

This allows us to express the beam size at the screen as a function of the Twiss parameters β_0 , α_0 , γ_0 at the reference point, given each quadrupole setting. A χ^2 -fit of σ given by Eq. (5) and (6) is then used to fit ε , β_0 and α_0 according to Eq. (9). Figure 1 shows an example of a quadrupole scan in the vertical plane.

RESULTS

To evaluate the performance of the quadrupole scan implementation, a set of 48 quadrupole scans were conducted. The scans aimed to compare the results of the estimated parameters at the start of the first quadrupole while scanning the current in different quadrupoles and observing the beam at different screens. A combined χ^2 -fit was made on the measurements of multiple scans, excluding obvious outliers mainly attributed to the uncertainty in the resolution limit correction, as discussed later. The combined χ^2 -fit enabled an estimate of the parameters that agreed well with a majority of measurements, which was then used as reference. The measured emittance in both planes of each scan is plotted in

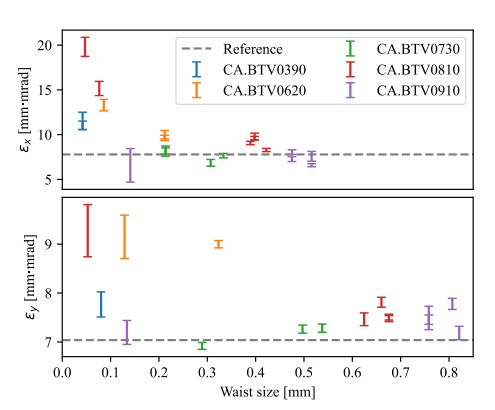


Figure 2: The measured emittance as a function of the standard deviation at the waist, with each color representing the screen used for measurements. The waist size value is calculated assuming the reference parameters are correct. Top: Horizontal plane. Bottom: Vertical plane.

Fig. 2, as a function of the minimum spot size predicted by the reference Twiss parameters.

Figure 2 shows that there is a clear trend of worsening results at lower waist sizes. This is mostly attributed to the uncertainty in screen resolution, as the outliers in measured emittance where very close to the estimated resolution limit given in Fig. 3. The results are also noticeably more reliable in the vertical plane. Due to all screens except one being slanted in the horizontal plane, the emitted light is more scattered in the horizontal image plane leading to a higher resolution limit, as seen in Fig. 3. In addition, the angle between the screen and the beam axis is also not entirely known, leading to uncertainty in the homographic calibration.

Beam Based Estimate of Screen Resolution Limit

From the large dataset of scans, it was possible to estimate the resolution limits of one screen (CA.BTV0180) that had a particularly wide discrepancy between the predicted and measured beam sizes. Figure 3 shows the discrepancy between the measured and predicted beam size, together with a least square fit of the resolution using Eq. (5). While contributions from dispersive [10] and chromatic [11] effects are not negligible, the consistency of this discrepancy over several months regardless of beam conditions and energy spread suggests that the majority of the measured size increase stems from the resolution limit.

Quadrupole Based Energy Measurements

The error in beam rigidity cannot be deduced from a quadrupole on a single screen, necessitating a separate energy measurement. However, since the focal length depends on the beam energy, a multiple-screen, multiple-optics approach allows us to infer the beam energy only using quadrupole scans.

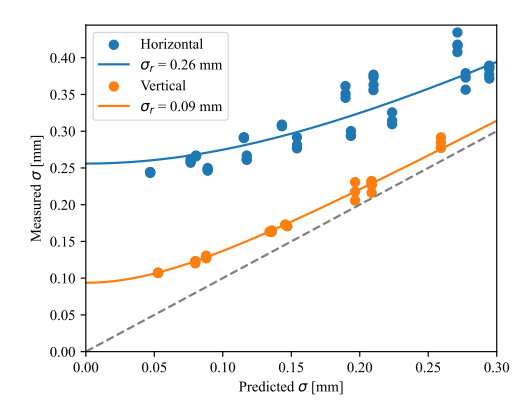


Figure 3: The measured beam size on CA.BTV0810 as a function of the beam size predicted using the reference beam parameters.

This approach was tested in simulation using a linear optics model, adding random measurement errors similar to those observed in practice. This yielded promising results, enabling a measurement of the energy within 1%. The results using real measurements were not as promising, with errors on the order of tens of MeV. This was attributed to systemic errors due to higher order effects introducing bias.

CONCLUSION AND OUTLOOK

The beam based measurement of resolution limit gave promising results but was ultimately not accurate enough without correction of dispersive [10] and chromatic [11] effects, which would be a logical next step in the development of the CLEAR quadrupole scans. Due to the difficulties in measuring the resolution limit, care should be taken during operation not to scan with beam sizes close to this limit. This also avoids dispersive effects. In operation, this can often be accomplished by scanning a quadrupole further upstream. On a longer time scale, it would be beneficial to install thinner YAG screens to lower the screen resolution limit

The approach of using a purely quadrupole-based energy measurement will be further studied. While the technique is time intensive and requires greater than usual care to avoid systemic errors in the beam size measurement, it does not require any change in beam orbit.

ACKNOWLEDGEMENTS

Presentation of this work at IPAC'25 was funded through the IPAC European Student Grant in cooperation with the Joint Universities Accelerator School. The author would also like to thank Eduard Prat for kindly addressing detailed questions regarding his publications from over a decade ago.

REFERENCES

- [1] D. Gamba et al., "The CLEAR user facility at CERN", Nucl. Instrum. Methods Phys. Res., Sect. A, vol. 909, pp. 480–483, Nov. 2018. doi:10.1016/j.nima.2017.11.080
- [2] R. Corsini *et al.*, "Status of the CLEAR user facility at CERN and its experiments", in *Proc. LINAC*'22, Liverpool, UK, 2022, pp. 753–757.
 doi:10.18429/JACOW-LINAC2022-THPOPA05
- [3] P. Korysko *et al.*, "The CLEAR user facility: a review of the experimental methods and future plans", in *Proc. IPAC'23*, Venice, Italy, 2023, pp. 876–879. doi:10.18429/JACOW-IPAC2023-MOPL141
- [4] R. Hartley and A. Zisserman, *Multiple view geometry in computer vision*, 2nd ed., Cambridge University Press, 2003.
- [5] A. H. Lumpkin et al., "Spatial resolution limits of YAG:Ce powder beam-profile monitors at the Fermilab A0 photoinjector," in Proceedings of FEL'09, Liverpool, UK, FEL Technology I: Accelerator, 2009, pp. 348–350.
- [6] I. Kandarakis et al., "On the response of Y₃Al₅O₁₂:Ce (YAG:Ce) powder scintillating screens to medical imaging

- X-rays," *Nucl. Instrum. Methods Phys. Res., Sect. A*, vol. 538, no. 1–3, pp. 615–630, Feb. 2005.
- [7] E. Prat, "Symmetric single-quadrupole-magnet scan method to measure the 2D transverse beam parameters," *Nucl. Instrum. Methods Phys. Res., Sect. A*, vol. 743, pp. 103–108, 2014.
- [8] E. Prat and M. Aiba, "Four-dimensional transverse beam matrix measurement using the multiple-quadrupole scan technique," *Phys. Rev. ST Accel. Beams*, vol. 17, p. 052801, 2014.
- [9] B. Holzer, "Beam optics and lattice design for particle accelerators," CAS - CERN Accelerator School: Advanced Accelerator Physics, Trondheim, Norway, 2013.
- [10] M. Castellano, A. Cianchi, and V. A. Verzilov, "Emittance and dispersion measurements at TTF," in *Proceedings of DIPAC'99*, *Chester, UK*, 1999, pp. 180–182.
- [11] E. Chiadroni *et al.*, "Chromatic effects in quadrupole scan emittance measurements," *Phys. Rev. ST Accel. Beams*, vol. 15, p. 082802, 2012.